

Energy Efficient IoT Sensor With RF Wake-Up and Addressing Capability

Hala Khodr^{ID}, Nour Kouzayha^{ID}, Mahmoud Abdallah, Joseph Costantine^{ID}, and Zaher Dawy^{ID}

Department of Electrical and Computer Engineering, American University of Beirut, Beirut 11-0236, Lebanon

Manuscript received September 19, 2017; revised October 3, 2017; accepted October 9, 2017. Date of publication October 3, 2017; date of current version November 2, 2017.

Abstract—In this article, we present a complete design for an optimized energy-efficient sensor for use in Internet of Things networks based on the concept of radio wake-up, with embedded addressing capability. Experimental and analytical results demonstrate the validity of the proposed design in terms of low power consumption and efficient functionality compared to existing solutions that are based on periodic wake-up patterns.

Index Terms—Sensor applications, internet of things, sensor networks, wake-up radio, energy efficiency, power consumption, sensor design.

I. INTRODUCTION

The Internet of Things (IoT) is a novel application venue for various fields [1]. IoT is based on low-cost low-power devices that are enabled for wireless communications. With the increase in the number of IoT devices, replacing or recharging batteries frequently is costly and infeasible. Traditionally, the problem of low power consumption has been addressed by duty cycling concepts [2]. Duty cycling consists of switching the main transceiver to sleep mode during pre-configured time intervals. While duty cycling saves power significantly, it severely limits the network reactivity. Recent advancements in hardware development have led to the birth of a new design paradigm of wake-up radios (WuRs) for further improvement in the reduction of power consumption [3]–[8]. WuRs minimize the unnecessary energy, as they activate the device only when there is a need. In a WuR architecture, an ultra-low power radio receiver (WuRx) and an address decoder are implemented to detect the wake-up signal, and to interrupt the device's micro-controller unit (MCU) to switch from sleep to active mode only when the received signal contains the address of the IoT device. Then, the MCU turns on the radio transceiver to initiate sensing and communications.

In this paper, an optimized architecture for an ultra-low power IoT sensor with radio wake-up is presented. An address decoder is developed to minimize false wake-up events. The performance of the proposed approach is analyzed analytically, verified experimentally and compared with existing solutions. The main novelty of our work is the end-to-end design approach taking into account various aspects of WuR-based sensor design. Such a design includes a wake-up receiver circuit, sensing elements, a communications interface, and an address decoder. The remainder of the paper is organized as follows; Section II presents the proposed sensor architecture. Section III presents implementation details with experimental results, comparison with existing solutions and analytical evaluation. Finally, Section IV concludes the paper.

II. PROPOSED ULTRA-LOW POWER IOT SENSOR

In this section, we present the different blocks of the proposed IoT sensor. The sensor is divided into four design components: wake-up circuit, address decoder, processing unit with sensing components, and communications interface.

Corresponding author: Nour Kouzayha (e-mail: nhk16@aub.edu.lb).

Associate Editor: Y. Duroc.

Digital Object Identifier 10.1109/LENS.2017.2762918

A. Wake-Up Circuit

The wake-up circuit functionality is to detect the wake-up signal and accordingly activate the MCU. It is composed of an antenna to pick up the RF signal, an impedance matching network to guarantee maximum power transfer, and a rectifier with a comparator to convert the RF power to dc voltage.

1) *Antenna and Wake-Up Signal*: The implemented antenna is a monopole antenna and has the following specifications: a frequency range between 2.4–2.5 GHz, a gain of 5 dBi, an SMA type connector with an impedance of 50 Ohms, omni-directional type radiation, and a length of 130 mm. The WuRx design should be of low power, hence, the modulation complexity must be kept low as well. The modulation used is on-off keying (OOK).

2) *Impedance Matching*: The impedance matching circuit matches the output impedance of the antenna to the input impedance of the rectifier. In our design, a single short-circuited stub matching network is used. This network is narrow-band and has relatively small size which leads to lower power losses and better sensitivity. In order to account for the parasitic effects of the diodes in the rectifying circuit and the tolerances of the dielectric constant of the substrate, a stub is included for post-fabrication tuning of the operating frequency. The tuning stub consists of a transmission line with a separate array of grounding vias. By varying the position of a capacitor along the line, the length of an equivalent RF short-circuited stub can be changed and the impedance of the rectifier can be controlled.

3) *Rectifier*: The rectifier's function is focused on eliminating the residual carrier signal while preserving the envelope of the received waveform. The rectifier used consists of a half-wave voltage doubler configuration. This configuration provides a higher dc voltage in comparison to a single diode rectifier and, hence, has better responsivity. The zero bias Schottky diode SMS7630 [9] is used. To ensure that the generated dc voltage reaches the comparator with minimal harmonic noise, a filter consisting of quarter-wavelength stubs at the fundamental, second, and third harmonics is designed and placed between the rectifier and the comparator. In addition, because the dc voltage of the rectifier is expected to have high ripple content, an RF bypass capacitor is added at the output to filter the ripples and enable a smooth dc voltage supply to the comparator.

4) *Comparator*: To step the rectifier low output voltage to a higher voltage capable of waking-up the MCU, the LTC1540 comparator [10] is added at the rectifier's output. It has a low quiescent current consumption and a built-in voltage reference of 1.13 V. Therefore, the power consumption is reduced since this reference is used instead of the battery for generating the threshold

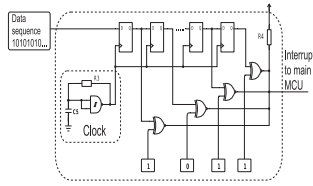


Fig. 1. Architecture of the address decoder.

voltage through a voltage divider. The minimum threshold to turn on the comparator is set to 50 mV, which is a reasonable level above any significant noise.

B. Address Decoder

The address decoder is a key subsystem that is responsible for decoding data received by the WuRx and generating a trigger only when the address is recognized. If the address decoder is not present, the MCU will wake-up at any 2.4 GHz signal, which increases the probability of false wake-up and causes unnecessary power loss. The designed address decoder (see Fig. 1) is an enhancement of the one proposed in [11]. The data received from the front-end circuit is processed into a shift register formed by a pipeline of D-flip-flops. Each flip-flop output is then compared to the corresponding bit in the saved address using XNOR gates. Once the data in the flip-flops matches the saved address, an interrupt is sent to the MCU. In our design, XNOR gates with open drain output are used and all the AND gates are replaced with a single pull up resistor, which minimizes the current consumption and the complexity of the developed circuit. Thus, our design differs from [11] where AND gates follow the output of XNOR gates for address match identification as indicated by their simulation analysis. In addition, in our work, a complete prototype is implemented and tested under realistic conditions.

C. Processing and Sensing Unit

The interrupt signal generated by the address decoder triggers the processing unit to wake-up. Once received, the processing unit reads data from its sensing inputs and forwards it to the destination. Therefore, the main blocks of this circuit are the processor and the linked sensing components.

1) *Processor*: We employ the Texas Instrument CC3200 launchpad unit which includes a wireless interface in addition to a micro-controller (MSP430) with an embedded antenna. This board has 1.8–3.6 V input voltage range, 4 μ A current consumption in the hibernate state, around 250 mA maximum current consumption, and up to 256 KB of RAM memory [12].

2) *Sensing Components*: The resistance temperature detectors (RTD) components are used for temperature and humidity sensing. Specifically, DHT-11 [13] is chosen as it outputs digital data which is recommended for the CC3200.

D. Communications Interface

The CC3200 offers an embedded WiFi interface that can be used to connect the sensor's MCU to a remote cloud server for data exchange and application layer functionality.

III. EXPERIMENTAL SETUP AND RESULTS

The prototype platform of the designed WuRx and address decoder are presented in Figs. 2 and 3, respectively. To verify the functionality of the WuRx, the reflection coefficient along with the dc output voltage and the sensitivity are determined by relying on the Agilent EE4438C ESG vector signal generator [14] that is transmitting a 1 W fixed signal. Later on, and in order

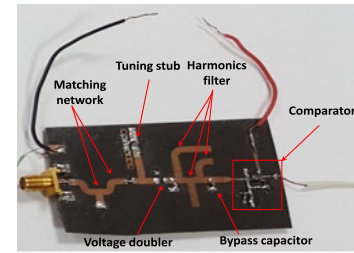


Fig. 2. Prototype of the wake-up receiver.

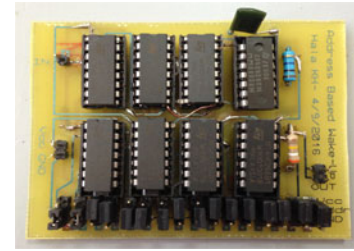


Fig. 3. Prototype of the address decoder.

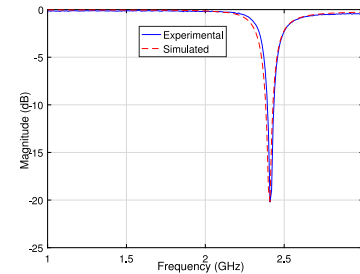


Fig. 4. S_{11} experimental vs simulated results.

to verify the functionality of the designed address decoder, the same signal generator is used to generate the 2.4 GHz OOK modulated signal carrying a 16-bit address. The reception of 1 corresponds to a 2.4 GHz signal with amplitude -25 dBm and duration 1 ms whereas the amplitude is set to -135 dBm to receive 0.

A. Impedance Matching and dc Output

A vector network analyzer is used to measure the reflection coefficient (S_{11}) at the input of the matching network. The position of the capacitor between the tuning stub and the via array plays an integral role in tuning the resonant frequency in order to achieve good agreement between measurements and simulations. Fig. 4 illustrates the consistency between the Advanced Design System (ADS) [15] simulation results and the experimental measurements. S_{11} 's magnitude is maximized at -20 dB at 2.4 GHz which verifies the impedance matching and the optimized power transfer. To measure the dc voltage at the output of the rectifier, the power received is varied from -30 to -15 dBm, and the dc output is measured at increments of 1 dBm. Fig. 5 demonstrates the voltage level variation before reaching the comparator in order to achieve the desired voltage level of 50 mV. Thus, the sensitivity of the system is around -28 dBm, which corresponds to maximum range of 22 m.

B. Data Measurements and Uploading

When the CC3200 receives an interrupt from the address decoder indicating a matched address, it senses temperature and humidity levels for around 30 sec and uploads to the cloud server over WiFi. After that, it goes into sleep mode until it receives an-

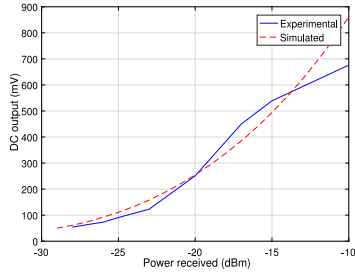


Fig. 5. Rectifier output versus power received.

Table 1. Measured current (μA) and power (μW) consumptions.

| Component | Active mode (μA) | Sleep mode (μA) | Active mode (μW) | Sleep mode (μW) |
|-----------------------|-------------------------------|------------------------------|-------------------------------|------------------------------|
| Wake-up receiver | 4.5 | 1.5 | 13.5 | 4.5 |
| Address decoder | 8.5 | 8.5 | 25.5 | 25.5 |
| Main micro-controller | 39500 | 4 | 118500 | 12 |

Table 2. Comparison of this work with other designs.

| | Power (μW) | Sens. (dBm) | Range (m) | Freq. (GHz) | Rate (kbps) | Latency (ms) |
|-----------|-------------------------|-------------|-----------|-------------|-------------|--------------|
| This work | 39 | -28 | 22 | 2.4 | 1 | 16.06 |
| [17] | 0.098 | -41 | 1.2 | 0.915 | 100 | - |
| [18] | 4.75 | -83 | 1200 | 0.868 | 0.128 | 484 |
| [19] | 26.4 | -53 | 41 | 0.868 | 2.7 | 13.08 |
| [11] | 13.41 | -54 | - | 0.868 | 100 | 0.08 |

other wake-up signal. In order to display the measured data in real time, a dashboard is implemented using Freeboard.io [16].

C. Current and Power Consumption Results

The current consumption of the IoT sensor is measured using a micro ammeter in the sleep and active modes as presented in Table 1. The WuRx consumes 4.5 μA of supply current at 3 V (13.5 μW) in the active mode and 1.5 μA (4.5 μW) in the sleep mode. On the other hand, the address decoder consumes 8.5 μA (25.5 μW) in both the active and the sleep modes. The main micro-controller CC3200 consumes 39.5 mA (118.5 mW) in the active mode and 4 μA (12 μW) in the sleep mode.

D. Latency

The latency of the complete sensor is computed as the sum of the latencies of the different components. Due to the comparator, the latency of the WuRx is 60 μs . As for the address decoder, the clock generator determines the latency of the circuit. The clock frequency is chosen as the double of the frequency at which we are sending data. The frequency of the transmitted signal is however limited to 1 KHz because of the used signal generator. Thus, the clock frequency is set to 2 KHz and the overall latency of the address decoder is equal to 16 ms when a 16 bits address is processed. On the other hand, the latency of the CC3200 and the communication interface is 20 ms.

E. Comparison With Existing Solutions

Table 2 presents the characteristics of the proposed wake-up circuit and address decoder compared to recent state of the art solutions. The solution with the lowest power consumption [17] (98 nW) has a lower sensitivity of -41 dBm but it does not support addressing which has a significant effect on its power consumption

Table 3. Current consumption and lifetime for scheduled and triggered schemes.

| Configuration | Scheduled $D_{\text{ON}} = 3.3\%$ | Triggered $D_{\text{ON}} = 3.3\%$ | Triggered $D_{\text{ON}} = 1.6\%$ | Triggered $D_{\text{ON}} = 0.83\%$ |
|-------------------------------|--------------------------------------|--------------------------------------|--------------------------------------|---------------------------------------|
| Consumption (μA) | 1307.3 | 1307.5 | 645.9 | 341.8 |
| Life time (days) | 56 | 55 | 113 | 213 |

and lifetime due to excessive false wake-ups. In addition, it has a low communication range (1.2 m). The solution with the highest sensitivity [18] (-83 dBm) also has a lower power consumption than our solution (4.75 μW); however, it has a very high latency of 484 ms which impacts its practicality for critical IoT scenarios. The solution presented in [19] has similar results to our solution for the power consumption (26.4 μW), latency (13.08 ms) and data rate (2.7 kbps), but a higher communication range (41 m) because it operates on a lower frequency band (868 MHz). Thus, it requires a larger antenna than ours which can impact the system design aspects. The designed address decoder is an enhancement of the one proposed in [11] with less complexity (AND gates are replaced with one pull-up resistor). However, [11] operates on a higher frequency (100 KHz instead of 1 KHz) and has a lower latency (0.08 ms compared to 16.06 ms). The limitation on the achieved latency is imposed by the available signal generator. However, with other signal generators, we can get similar latency as [11] with less components and current consumption.

F. Sensor Life Time Results

The lifetime is a critical parameter of a sensor since it directly affects the long-term costs of its network. We have powered our IoT sensor by two standard AA alkaline batteries with a capacity of 2500 mAh. Assuming that we have the full charge of the battery at our disposal, the maximum lifetime T can be calculated as follows:

$$T = \frac{C_{\text{bat}}(\text{mAh})}{I_{\text{Total}}(\text{mA})} \times 0.7 \quad (1)$$

where C_{bat} is the battery capacity and I_{Total} is the current consumption. Equation (1) includes a multiplication factor of 0.7 which accounts for the external factors that affect the estimated time [20]. Based on the measured current consumption values presented in Table 1, the proposed sensor has a theoretical standby time of about 14 years. In case of continuous active mode operation, the maximum lifetime reaches about 2 days. Despite the fact that the active consumption of the sensor is high, the sensor is only active occasionally and for a short time for the majority of IoT applications.

To evaluate the performance of the proposed “triggered wake-up” sensor, we compare it with the standard “scheduled wake-up” sensor that employs the duty cycling technique. Note that the “scheduled wake-up” sensor does not require a WuRx or an address decoder since the MCU is internally programmed to wake-up. The time during which the sensor wakes-up and communicates is called active cycle time T_{ON} and is set to 1 min for both scheduled and triggered wake-ups. The sleep cycle of the scheduled wake-up sensor T_{schedule} is set to 0.5 hours. In contrast, the triggered wake-up sensor has several values of the sleep cycle T_{trigger} corresponding to different types of IoT applications, with T_{trigger} of {2, 1, 0.5} hours, i.e., it remains awake 0.83%, 1.6%, and 3.3% of the time, respectively. Therefore, the overall current consumption is

$$I_{\text{Total}} = D_{\text{ON}} \cdot I_{\text{ON}} + (1 - D_{\text{ON}}) \cdot I_{\text{sleep}} \quad (2)$$

where D_{ON} is the percentage of active per total lifetime, and I_{ON} and I_{sleep} are the average current consumptions in active and sleep modes, respectively. Results of the triggered wake-up sensor, presented in Table 3, demonstrate the potential for significant gains

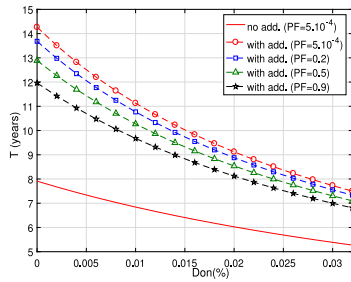


Fig. 6. Lifetime as function of D_{ON} .

over the scheduled wake-up sensors. With shorter active time percentage ($D_{ON} = 0.83\%$), the triggered wake-up scheme achieves an even greater improvement, with energy savings ranging up to four orders of magnitude. This translates in estimated lifetimes that are much longer than those achievable in sensors with scheduled cycles. The lifetime of the triggered wake-up sensor is slightly smaller than the scheduled wake-up sensor with the same active time percentage ($D_{ON} = 3.3\%$) because of the extra power consumption of the WuRx and address decoder.

G. Address Decoding and False Wake-Up Analysis

To evaluate the benefits of the address decoder circuit, we compare the battery lifetime of our proposed IoT sensor with address decoder to a standard broadcast-based IoT sensor (excluding the address decoder) for different false wake-up probabilities. When a false wake-up occurs, the WuRx and the address decoder become active. However, since the address is not matched, the address decoder does not interrupt the MCU. Thus, there are basically three different scenarios with the following consumptions:

$$I_{ON} = I_{WuR,ON} + I_{add,ON} + I_{MCU,ON} \quad (3)$$

$$I_F = I_{WuR,ON} + I_{add,ON} + I_{MCU,sleep} \quad (4)$$

$$I_{sleep} = I_{WuR,sleep} + I_{add,sleep} + I_{MCU,sleep} \quad (5)$$

where I_F is the total current consumption when a false wake-up event occurs and $I_{WuR,ON}$, $I_{add,ON}$, $I_{MCU,ON}$ correspond to the current consumptions of the WuRx, address decoder, and MCU in active mode, and $I_{WuR,sleep}$, $I_{add,sleep}$, and $I_{MCU,sleep}$ in sleep mode, respectively. The total current consumption of the IoT sensor with the added address decoder is derived below as function of the active time percentage D_{ON} , as well as the probability of false wake-ups P_F :

$$I_{Total} = D_{ON} \cdot I_{ON} + (1 - D_{ON}) \cdot P_F \cdot I_F + (1 - D_{ON}) \cdot (1 - P_F) \cdot I_{sleep} \quad (6)$$

Fig. 6 depicts the estimated sensor lifetime T as a function of D_{ON} for the false wake-up probabilities $5 \cdot 10^{-4}$, 0.2, 0.5, and 0.9. The WuRx without addressing falsely wakes-up the MCU causing extra power consumption and reducing the overall lifetime of the sensor. For instance, an IoT sensor following a nominal active time percentage of 0.02% and operating with no addressing capability with a false wake-up probability of $5 \cdot 10^{-4}$ lasts no longer than six years. Nevertheless, the IoT sensor is capable of extending the network lifetime to nine years with same false wake-up probability and active time percentage if it is equipped with the proposed address decoder. Even when P_F increases, the IoT sensor with addressing achieves better battery lifetime compared to the broadcast-based IoT sensor.

IV. CONCLUSION

In this article, we present a complete design of an IoT sensor, starting from the radio wake-up receiver to the addressing decoder and ending by the micro-controller, the communications interface

and the sensing components. The design techniques are supported by analytical models, combined with simulations and experiments to better define the achievable trade-offs. As IoT applications require addressing capabilities to minimize the false wake-up rate, the proposed design compares the received data to a stored address to perform address detection. We present various performance results to validate our design and demonstrate its superiority over the scheduled wake-up approach in terms of energy reduction gains.

ACKNOWLEDGMENT

This work was supported by the Ph.D. Scholarship from the National Council for Scientific Research of the Lebanese Republic and the American University of Beirut. The statements made are solely the responsibility of the authors.

REFERENCES

- [1] A. Al-Fuqaha, M. Guizani, M. Mohammadi, M. Aledhari, and M. Ayyash, "Internet of things: A survey on enabling technologies, protocols, and applications," *IEEE Commun. Surveys Tut.*, vol. 17, no. 4, pp. 2347–2376, Oct.–Dec. 2015.
- [2] I. Demirkol, C. Ersoy, and E. Onur, "Wake-up receivers for wireless sensor networks: Benefits and challenges," *IEEE Wireless Commun.*, vol. 16, no. 4, pp. 88–96, Aug. 2009.
- [3] N. Kouzayha, Z. Dawy, and J. G. Andrews, "Analysis of a power efficient wake-up solution for M2M over cellular using stochastic geometry," in *Proc. IEEE Globecom Conf.*, Washington, DC, USA, Dec. 2016, pp. 1–7.
- [4] J. Blanckenstein, J. Klaue, and H. Karl, "A survey of low-power transceivers and their applications," *IEEE Circuits Syst. Mag.*, vol. 15, no. 3, pp. 6–17, Jul.–Sep. 2015.
- [5] C. Shekhar, S. Varma, and M. Radhakrishna, "A passive wake-up circuit for event driven wireless sensor network applications," *J. Circuits Syst. Comput.*, vol. 24, no. 8, 2015, Art. no. 1550120.
- [6] L. Chen, J. Warner, W. Heinzelman, and I. Demirkol, "MH-REACH-Mote: Supporting multi-hop passive radio wake-up for wireless sensor networks," in *Proc. IEEE Int. Conf. Commun.*, Jun. 2015, pp. 6512–6518.
- [7] T. Taris, H. Kraimia, D. Belot, and Y. Deval, "An FSK and OOK compatible RF demodulator for wake up receivers," *J. Low Power Electron. Appl.*, vol. 5, no. 4, pp. 274–290, 2015.
- [8] M. Magno, V. Jelicic, B. Srinovski, V. Bilas, E. Popovici, and L. Benini, "Design, implementation, and performance evaluation of a flexible low-latency nanowatt wake-up radio receiver," *IEEE Trans. Ind. Informat.*, vol. 12, no. 2, pp. 633–644, Apr. 2016.
- [9] SMS7630, SKYWORKS, Woburn, MA, USA, May 2015. [Online]. Available: http://www.skyworksinc.com/uploads/documents/SMS7630_061_201295H.pdf
- [10] LTC1540 nanopower comparator with reference, Linear Technol. Corp., Milpitas, CA, USA. 1997. [Online]. Available: <http://www.linear.com/product/LTC1540>
- [11] Y. Ammar, S. Bdiri, and F. Derbel, "An ultra-low power wake up receiver with flip flops based address decoder," in *Proc. 12th Int. Multi-Conf. Syst. Signals Devices*, Mar. 2015, pp. 1–5.
- [12] CC3200 simpleLink Wi-Fi, Texas Instrument, Dallas, TX, USA, Feb. 2015. [Online]. Available: <http://www.ti.com/lit/ds/symlink/cc3200.pdf>
- [13] DHT11 humidity & temperature sensor, D-Robotics, Jul. 2010. [Online]. Available: <http://www.micropik.com/PDF/dht11.pdf>
- [14] Agilent E4438C ESG vector signal generator data sheet, Agilent Technologies, Santa Clara, CA, USA. May 2012. [Online]. Available: <http://literature.cdn.keysight.com/litweb/pdf/5988-4039EN.pdf>
- [15] Keysight EEs0f EDA advanced design system, Keysight Technologies, Santa Rosa, CA, USA. Jul. 2017. [Online]. Available: <http://literature.cdn.keysight.com/litweb/pdf/5988-3326EN.pdf>
- [16] Freeboard.io: Ridiculously simple internet of things tools and solutions, Bug Labs, New York, NY, USA. [Online]. Available: <http://freeboard.io/> Accessed on: 5 Jan., 2016.
- [17] N. E. Roberts and D. D. Wentzloff, "A 98 nW wake-up radio for wireless body area networks," in *Proc. IEEE Radio Freq. Integr. Circuits Symp.*, Jun. 2012, pp. 373–376.
- [18] H. Milosiu *et al.*, "A 3 μ W 868-MHz wake-up receiver with –83 dBm sensitivity and scalable data rate," in *Proc. Eur. Solid-State Circuits Conf.*, Bucharest, Romania, Sep. 2013, pp. 387–390.
- [19] J. Oller, I. Demirkol, J. Casademont, J. Paradells, G. U. Gamm, and L. Reindl, "Performance evaluation and comparative analysis of subcarrier modulation wake-up radio systems for energy-efficient wireless sensor networks," *Sensors*, vol. 14, no. 1, pp. 22–51, 2014.
- [20] Digi-Key Electronics, Thief River Falls, MN, USA. [Online]. Available: <http://www.digikey.com/en/resources/conversion-calculators/conversion-calculator-battery-life>. Accessed on Nov. 22, 2015.